Stretching of single DNA molecules caused by accelerating flow on a microchip

Ken Hirano, Takafumi Iwaki, Tomomi Ishido, Yuko Yoshikawa, Keiji Naruse, and Kenichi Yoshikawa

Citation: The Journal of Chemical Physics **149**, 165101 (2018); doi: 10.1063/1.5040564
View online: https://doi.org/10.1063/1.5040564
View Table of Contents: http://aip.scitation.org/toc/jcp/149/16
Published by the American Institute of Physics

Stretching of single DNA molecules caused by accelerating flow on a microchip

Ken Hirano,[1] Takafumi Iwaki,[2,a)] Tomomi Ishido,[1] Yuko Yoshikawa,[3] Keiji Naruse,[4] and Kenichi Yoshikawa[1,3]

[1]*Health Research Institute, National Institute of Advanced Industrial Science and Technology (AIST), Takamatsu, Kagawa 761-0395 Japan*
[2]*Faculty of Medicine, Oita University, Yufu, Oita 879-5593, Japan*
[3]*Faculty of Life and Medical Science, Doshisha Universiy, Kyotanabe, Kyoto 610-0321, Japan*
[4]*Graduate School of Medicine, Dentistry and Pharmaceutical Sciences, Okayama University, Okayama 700-8558, Japan*

(Received 18 May 2018; accepted 24 September 2018; published online 23 October 2018)

DNA elongation induced by fluidic stress was investigated on a microfluidic chip composed of a large inlet pool and a narrow channel. Through single-DNA observation with fluorescence microscopy, the manner of stretching of individual T4 DNA molecules (166 kbp) was monitored near the area of accelerating flow with narrowing streamlines. The results showed that the DNA long-axis length increased in a sigmoidal manner depending on the magnitude of flow acceleration, or shear, along the DNA chain. To elucidate the physical mechanism of DNA elongation, we performed a theoretical study by adopting a model of a coarse-grained nonlinear elastic polymer chain elongated by shear stress due to acceleration flow along the chain direction. https://doi.org/10.1063/1.5040564

I. INTRODUCTION

Along with the recent development of microfabrication technology, microfluidics has become a powerful tool for manipulating micrometer-scale soft materials, such as cells[1] and giant DNA molecules.[2–4] Microfluidic techniques are important not only in the field of engineering but also in the field of medical and biological science.[5–7] In particular, microchannels are frequently used to study the mechanical properties of these substances.[8]

A soft material is easily deformed as a result of interactions with a fluid. The key to understanding such deformation is the concept of extensional flow,[9,10] which refers to outflow from a stagnation point associated with opposing inflow. For example, standard shear flow induces the ellipsoidal deformation of a cell.[11] This is because a shear flow field is a combination of extensional and rotational flows.[10] For a polymeric molecule, elongation of the chain, which is called the coil-stretch transition, occurs under extensional flow.[9,10]

The coil-stretch transition has been examined indirectly as a macroscopic property.[12–14] For example, the viscosity of a polymer solution increases abruptly at a certain shear rate,[12] which suggests that a polymer molecule is distinctively stretched at that point. In the 1990s, visualization of a monomolecular DNA chain by fluorescent microscopy enabled the direct measurement of the interplay between flow and an individual polymeric chain with one pinned end.[15] This observation of the direct response of a DNA chain to an applied force supported the proposal of a theoretical equation of elasticity for a long-chain DNA molecule.[16,17]

Subsequently, the behavior of DNA in planar extensional flow using a cross-slot device was investigated to better understand the coil-stretch transition.[18,19] Similar experiments were performed with simple shear flow[20,21] and mixed flow,[22] which resulted in rather gentle stretching compared with planar extensional flow. A cross-slot devise has now become an important tool for elongating a monomolecular DNA chain.[23,24]

In the present paper, we studied the effect of extension on the conformation of long DNA molecules under the acceleration of flow with situational pumping of a sample solution, by adopting an apparatus in which a large inlet pool is connected to a narrow channel (Fig. 1). Despite the above-mentioned studies on the change in conformation under shear flow including the coil-stretch transition, our understanding of shear flow under acceleration of fluid velocity seems to be in a primitive stage, both theoretically and experimentally. We also performed a theoretical study of DNA elongation caused by a microfluidic flow, by adopting a coarse-grained model of a nonlinear elastic continuous chain under a flow field with a constant shear rate. This model predicts a kind of sigmoidal effect on the extension of DNA molecules, which corresponds well to the experimental trend in the present study.

II. MATERIALS AND METHODS

A. Sample preparation

T4 GT7 DNA (166 kbp, Nippon Gene, Japan) was stained with the intercalating dye YOYO-1 at a dye-to-base pair ratio

a)Author to whom correspondence should be addressed: iwaki48@oita-u.ac.jp

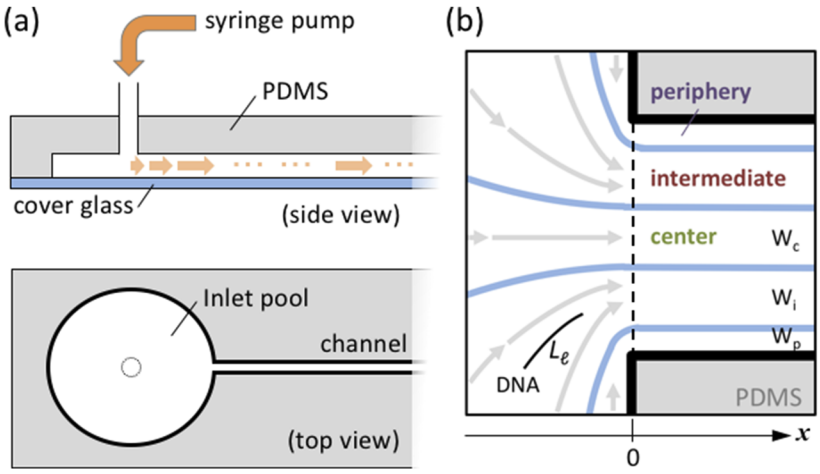

FIG. 1. (a) Geometry of the PDMS microfluidic chamber, to which the sample solution was continuously supplied with a syringe pump through a hole leading into the inlet pool. (b) Schema of the flow field, where the diameter of the inlet pool was 5 μm and the width of the microchannel was 100 μm under a depth of 20 μm for the entire flow system. DNA stretching was analyzed by considering three different flow regions: center (20 μm wide: W_c), intermediate (30 μm wide: W_i), and periphery (10 μm wide: W_p). The long-axis length of the elongated DNA molecule is denoted as L_l.

1:46. The stained DNA solution was diluted to 165 pg/μL with the running solution consisting of 20 mM Tris-HCl buffer pH 7.4 and 30% (v/v) glycerol (Sigma-Aldrich).

B. Instrumentation and measurement

To investigate the stretching of single DNA molecules, we used a microfluidic chip made of poly(dimethylsiloxane) (PDMS), which has one microchannel (100 μm wide, 20 μm deep, 20 mm long) with an inlet reservoir (5 mm in diameter) [Fig. 1(a)]. DNA solution was injected into the inlet reservoir and microchannel with a syringe microinjection pump (model CMA/100, CMA Microdialysis AB, Sweden) through a 2 mm tube. The flow rate inside the microfluidic chip could be controlled within a range of 50–500 μm/s.

Fluorescent images of single DNA molecules and beads were obtained using an inverted microscope (IX70, Olympus, Japan) equipped with a 100x, NA 1.3 objective lens and a electron multiplying charge coupled device (EM-CCD) camera (Hamamatsu Photonics, Japan). The captured images were recorded on a personal computer (PC). DNA stretching was investigated near the boundary between the inlet reservoir and the microchannel. As shown in Fig. 1(b), we analyzed the elongation of DNA molecules under an acceleration-flow field by considering three different stream regions: center (20 μm wide: W_c), intermediate (30 μm wide: W_i), and periphery (10 μm wide: W_p). The length and velocity of DNA in recorded images were analyzed using Meta Imaging Software (Molecular Devices, USA). In the measurement of DNA length, the position of the rear terminus of a stretched DNA molecule was defined as position x on the channel axis. The ensemble statistics of T4 DNA stretching were investigated for about 200 molecules passing through the connection.

III. RESULTS

First, throughout the study, we used a 30% glycerol solution because DNA molecules exhibit greater elongation under fluid flow than in the absence of glycerol (see the supplementary material). In addition, DNA maintains a B-form secondary structure in 30% glycerol solution.

Figure 2(a) exemplifies the change in the long-axis length L_l in the x direction, together with fluorescence images, in three different regions: center, intermediate, and periphery. Here, the position $x = 0$ is at the connection between the inlet pool and the narrow channel, and a stretched DNA molecule was defined to have its rear terminus at position x. Elongation of a single DNA molecule was observed at a flow speed of 300 μm/s measured at the zero position. DNA molecules

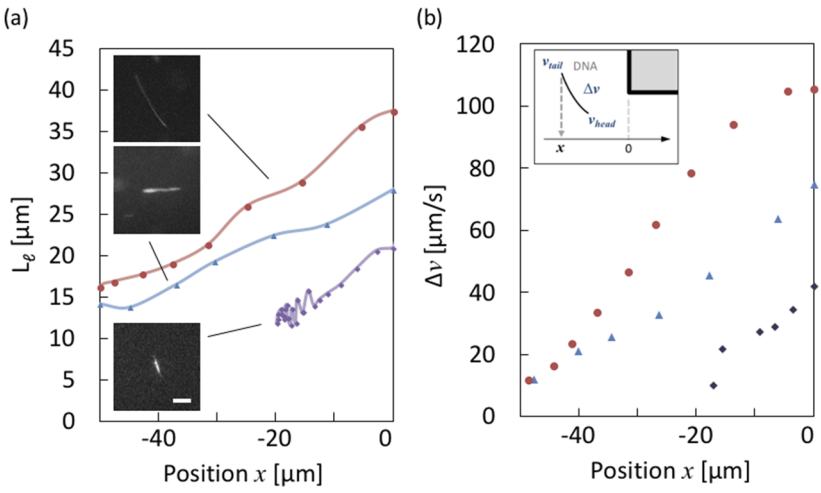

FIG. 2. (a) Change in the long-axis length L_l of a T4 DNA molecule depending on the position x in the apparatus, together with fluorescent images. Scale bar: 10 μm. (b) Difference in velocity Δv between the head and tail of a T4 DNA molecule versus position x. Inset: The x-axis is along a channel axis. The position $x = 0$ corresponds to the connection between an inlet pool and a channel. Δv is the difference between the velocities of the head (v_{head}) and tail (v_{tail}) termini of an elongating DNA molecule. Each measurement in (a) and (b) was carried out in the central (blue triangle), intermediate (red circle), and peripheral (purple rhombus) regions. The flow speed was 300 μm/s.

were observed to drift toward a microchannel accompanied by a gradual increase in L_l along the streamlines. In photographs, DNA molecules appear as almost straight single molecules. L_l was measured from captured fluorescent images. In our experiments, a pale afterimage appears with a comet shape according to flow speed, and these afterimages were well distinguishable from original objects for the time-successive measurements with video analysis. As exemplified in the figure, we observed a general experimental trend that DNA elongation is pronounced mostly for the intermediate region compared to the central and peripheral regions. For short L_l in the peripheral region, L_l was slightly disturbed due to the Brownian motion of gently stretched coiled-state DNA by low shear force. The velocity difference Δv between the termini of a single DNA molecule was also investigated in terms of position relative to the connection [Fig. 2(b)]. Δv is defined as $\Delta v = v_{head} - v_{tail}$, where v_{head} and v_{tail} are the velocities of the head and tail termini of an elongated DNA molecule drifting toward the channel entrance, respectively [Fig. 1(b)]. The properties of Δv in any region correspond to the DNA elongation properties in Fig. 2(a). It is clear that the flow speed increases linearly along the channel axis toward the connection. L_l almost perfectly follows the rise in the flow speed. As the flow speed inside the channel only rises in the vicinity of the connection, L_l clearly decreased after the flow speed became constant. This indicates that a single DNA molecule near the connection undergoes quite large tension. In addition, the DNA molecules did not reach a fully relaxed coiled state due to the presence of simple shear[20,21] from the wall. Based on the findings in Figs. 2(a) and 2(b), we found that both termini of DNA molecules accelerated while drifting. This implies that the flow speed accelerates along streamlines near the connection, and this speed difference causes DNA stretching. Δv of the intermediate region showed a large change compared to those in the other regions. Hereafter, we discuss DNA molecules in the intermediate region, which are effectively stretched using our system.

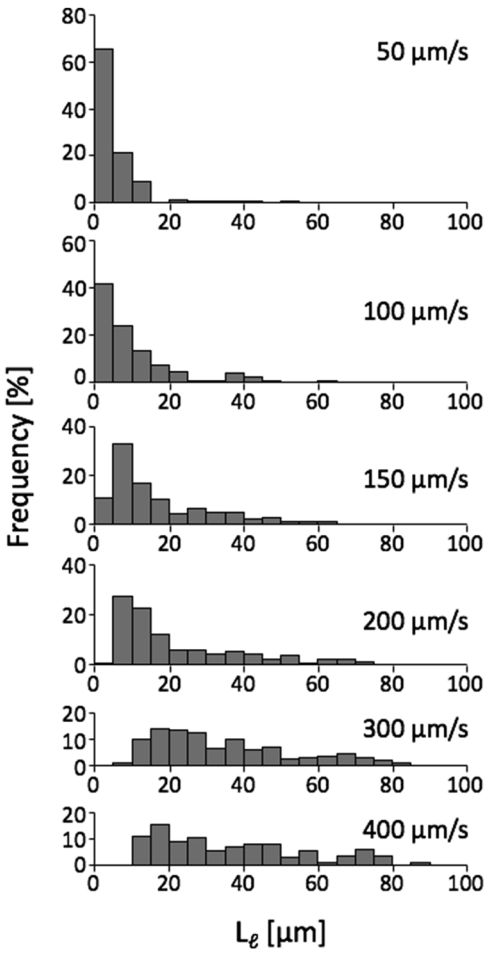

FIG. 3. Histograms of DNA long-axis length L_l in the intermediate region for various flow speeds. About 200 stretched DNA molecules were measured for each histogram.

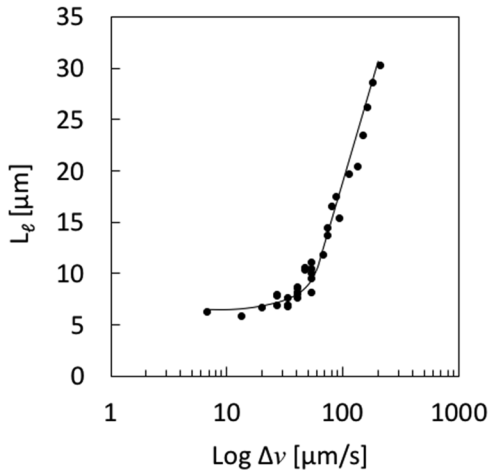

FIG. 4. Change in the long-axis length L_l of DNA versus Δv, the difference in velocity between the head and tail of a DNA molecule.

Figure 3 shows histograms of the DNA long-axis length L_l for various flow speeds at the connection. L_l values for individual DNA molecules were measured when their front terminus came to the connection. With a flow speed of 50 μm/s, more than half the molecules have lengths below 5 μm. Nevertheless, a small fraction of molecules have lengths comparable to their entire length. When the flow speed increases, the population of stretched DNA grows gradually. Moreover, overstretched molecules (longer than 56 μm) appear even with a relatively slow flow (100 μm/s). With a flow speed of 400 μm/s, overstretched molecules reach a length of 1.6 times the entire length in the absence of flow. In such fast flow, however, DNA molecules show a wide range of lengths, from 5 μm to 90 μm. In fact, the mean value of L_l is still about 40 μm under this condition.

Figure 4 shows the long-axis length L_l versus Δv for single DNA molecules. The experimental conditions are the same as those in Fig. 2. There seems to be a threshold for Δv in DNA elongation. It is clear that L_l increases with a rise in Δv. This implies that Δv causes DNA stretching.

IV. DISCUSSION

The DNA long-axis length increases depending on the degree of flow acceleration and the resulting shear stress along the DNA chain (Figs. 3 and 4). If we consider the highly fluctuating nature of a giant DNA molecule at room temperature, it is argued that accelerated flow into a microchannel

dramatically stretches a long DNA chain. The presence of short DNA under a fast flow can be attributed to original fragmented DNA. In fact, it can be confirmed that small fragments were mixed in the sample solution as shown in Fig. S4. On the other hand, it is noted that DNA molecules larger than the natural length, 56 μm, appeared under an accelerating flow. It is known that YOYO-1 dye as a bis-intercalator elongates DNA by 40%-50% at a maximum (around a dye-to-base pair ratio of 1:1). Meanwhile, our samples were prepared with a staining ratio as 1:50. From the results of the reported literature,[25,26] an increase in contour lengths of DNA molecules by dye binding is estimated to be ~3% in our experimental conditions. Thus, the longer DNA chains above the length of 56 μm observed along the accelerating shear flow are attributable to overstretched DNA molecules transformed from the B-form.

The simplest model of a long polymer in a flow field would be a dumbbell model, where two beads are joined by a nonlinear elastic spring.[27] An N-bead model can take into account a more detailed interaction between a chain conformation and a fluid structure, which has been frequently adopted in simulation studies.[27,28] A coarse-grained nonlinear elastic chain model is developed as a natural extension of the N-bead model. Below, a one-dimensional version of this coarse-grained model is formulated.

Here we introduce the coordinate λ along the cylindrical axis of a smeared extended DNA chain where $\lambda = 0$ at the mid-point of the chain. In a steady state in a center-of-mass system, the balance between a slip friction per unit area $\sigma(\lambda)$ and the local tension of a DNA chain $\tau(\lambda)$ leads to the following equation:

$$\frac{\mathrm{d}\tau}{\mathrm{d}\lambda} + \pi D\sigma = 0, \tag{1}$$

where D is the effective diameter of the smeared polymer. The boundary condition is $\tau = 0$ at the end points of the DNA molecule. As shown in Fig. 2(a), the flow speed near the entrance increases linearly over a wide region. If the flow speed is not large, $\sigma(\lambda)$ may be given by a linear equation $\sigma(\lambda) = \chi\dot{\gamma}\lambda$, where χ is a friction coefficient and $\dot{\gamma}$ is the shear rate. (The Reynolds number is estimated as vw/ν for a channel and $vL^2/(\nu w)$ for a DNA molecule, where v is a flow speed, w is the channel width, L is DNA contour length, and ν is a dynamic viscosity. For a flow speed 400 μm/s, the Reynolds numbers are 2×10^{-2} and 6×10^{-3}, respectively.) In this case, the local tension obeys the following equation:

$$\tau = -\frac{1}{2}\pi\chi\dot{\gamma}D\lambda^2 + \tau_{\mathrm{M}}, \tag{2}$$

where τ_{M} is an integral constant. At the end-points of DNA, local tension must be zero. Thus, the positions of the end-points $\lambda = \pm\lambda_{\mathrm{M}}$ are obtained as follows:

$$\lambda_{\mathrm{M}} = \sqrt{\frac{2\tau_{\mathrm{M}}}{\pi\chi\dot{\gamma}D}}. \tag{3}$$

A similar relation for local tension is derived for a DNA molecule stretched in a cross-slot device.[24] In this device, the flow velocity changes almost linearly near the stagnation point at the center of the cross-slot over the channel width.[3,24] On the other hand, the flow velocity in each slot is constant regardless of the distance from the stagnation point. Thus, for a very long DNA stretched over the whole channel, local tension can be approximated by a triangular curve[24] rather than a parabolic curve as in Eq. (2).

To relate tension to elongation, we adopt the following interpolation formula for a force-extension curve for DNA:[16,24,29]

$$\tau = \frac{k_BT}{l_{\mathrm{p}}}\left[r + \frac{1}{4(1-r)^2} - \frac{1}{4}\right], \tag{4}$$

where l_{p} is the persistence length and r ($0 \le \mathrm{r} \le 1$) is the actual length R over the contour length L. While a topological variance such as supercoiling/denaturation makes a force-extension curve more complicated,[30] Eq. (4) is valid for a relatively wide range of conditions, unless the applied force is too strong. In a coarse-grained model, r may be replaced by local stretching $d\lambda/ds$, where s is the coordinate along the contour. Equations (2) and (4) then give $d\lambda/ds$ as a function of λ and τ_{M}. This equation system closes with the following equation for mass conservation:

$$\int_0^{\lambda_{\mathrm{M}}} 1/\left(\frac{\mathrm{d}\lambda}{\mathrm{d}s}\right)\mathrm{d}\lambda = \frac{L}{2}. \tag{5}$$

Unfortunately, Eq. (4) leads to a logarithmic divergent term in Eq. (5) in the limit of $\lambda \to \lambda_{\mathrm{M}}$. This is because Eq. (4) allows for an infinite-density polymer in the absence of external force. To avoid such divergence, it is helpful to introduce an entropic decrease due to the confinement to the free energy of the ideal chain as follows:[31]

$$F_{\mathrm{ideal}} = \frac{3}{2}k_BT\left(\alpha^2 + \alpha^{-2}\right), \tag{6}$$

where F_{ideal} is the free energy of the ideal chain and $\alpha = R/\sqrt{Ll_K}$ is an expansion factor of the chain, where l_{K} is the Kuhn length. When l_{K} is taken to be $2l_{\mathrm{p}}$, this entropic decrease modifies the tension-extension relation [Eq. (4)] as follows:

$$\tau = \frac{k_{\mathrm{B}}T}{l_{\mathrm{p}}}\left[r - 6\frac{{l_{\mathrm{p}}}^2}{L^2}r^{-3} + \frac{1}{4(1-r)^2} - \frac{1}{4}\right]. \tag{4'}$$

To solve λ_{M}, we first assume that D takes a constant value. In the limit of no shear, the radius of a smeared chain can be evaluated by the radius of gyration of an ideal chain $R_{\mathrm{g}} = \sqrt{Ll_{\mathrm{p}}/3}$. If the flow cannot penetrate the chain region, the surface area exposed to the slip is $2\pi R_{\mathrm{g}}\mathrm{d}\lambda$ times the volume fraction of the chain $\pi a^2\mathrm{d}s/(\pi {R_{\mathrm{g}}}^2\mathrm{d}\lambda)$, where a is the polymer thickness, and in this case, a DNA helix has a radius of 1 nm, and $d\lambda/ds = \sqrt{L/l_{\mathrm{p}}}$. Thus, the effective diameter is evaluated as

$$D = 2\sqrt{3}a^2/l_{\mathrm{p}}. \tag{7}$$

Figure 5 shows a plot of polymer elongation ($2\lambda_{\mathrm{M}}$) versus dimensionless shear rate $\Gamma = \chi\dot{\gamma}al_{\mathrm{p}}L^2/(k_{\mathrm{B}}T)$. The persistence length and contour length of the molecule are set to be 50 nm and 56 μm, respectively. When the shear rate is very small, the molecule is not elongated at all. Between $\Gamma = 1.116 \times 10^3$ and 1.117×10^3, a singular behavior is observed. Polymer elongation seems to jump discontinuously within this region. This indicates that the elongation of a long polymer chain

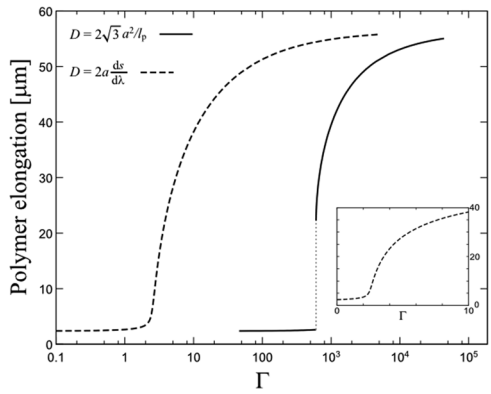

FIG. 5. Theoretical curve of polymer elongation ($2\lambda_M$) in a steady state versus a dimensionless shear rate Γ. D is the effective diameter of the molecule, l_p is the persistence length (50 nm), and a is the polymer thickness (1 nm). The contour length of the molecule is set to be 56 μm. The inset shows the same plot with a linear scale.

along a shear gradient may occur in an on/off manner. Once the molecule is elongated, its long-axis length asymptotically approaches the contour length (fully stretched state) with an increase in the shear rate.

Unfortunately, such discontinuous behavior is not seen in the experimental curve shown in Fig. 4. This suggests that the effective diameter is not constant, but rather depends on local stretching. Here we consider the simplest case where the effective diameter D is in proportion to local stretching $d\lambda/ds$. For example, in fully penetrating flow, all monomer units are exposed to the flow, and the exposed surface area is given by $2\pi a ds$. This leads to the following equation for the effective diameter:

$$D = 2a\frac{\mathrm{d}s}{\mathrm{d}\lambda}. \tag{8}$$

Instead of Eq. (2), Eqs. (1) and (8) lead to the following equation:

$$\tau = -2\pi a\chi\dot{\gamma}\left(\frac{\lambda_M L}{2} - \lambda s - \int_{\lambda}^{\lambda_M} s\mathrm{d}\lambda\right). \tag{2'}$$

A solution of this revised equation is also plotted in Fig. 5. Since the friction coefficient χ is unknown, a comparison of Γ at the transition point would not be very meaningful. Here we focus on an argument regarding the nature of the coil-stretch transition. For fully penetrating flow, the transition occurs continuously. In particular, a stretched DNA <22 μm is stably observed in this condition, unlike the case where the effective diameter is constant. The present experimental result supports the notion that flow fully penetrates into the coiled structure of DNA.

The theoretical curves in Fig. 5 represent a steady state for the polymer configuration. Under a constant shear rate, a polymeric chain in a coiled state would undergo relaxation to give a steady stretched form. In the present study, a DNA molecule passed an accelerating region within 1 s (data not shown). The relaxation time of a monomolecular DNA of this size (without shear) is estimated to be on the order of 10 s[32,33] In addition, the relaxation time is known to increase near the coil-stretch transition point.[34,35] On the other hand, the shear rate itself decreases the relaxation time. For example, the untucking of a twofold chain has been suggested to proceed at a pace in proportion to the shear rate.[36]

A numerical simulation of 40 beads linked by springs resembling 10^6 Da polyethylene oxide (PEO) has been reported,[37] where the plot of PEO chain extension versus Deborah number in the steady state was quite similar to our theoretical curve for a fully penetrating flow. T4 DNA stretching experiments with a cross-slot device also reported a similar experimental trend.[38]

Polymer configurations under shear have been discussed for various conditions. Panja *et al.* stated that a short DNA segment undergoes a buckling transition above a critical Weissenberg number (corresponding to Γ in the present paper).[39] This transition proceeds continuously with a change in the Weissenberg number because buckling results in a decrease in the compressing force.

By contrast, under shear parallel to a flow, elongation increases the total viscous force applied to the molecule. If this increase overwhelms the increase in elastic force, stretching induces further stretching, and thus, the polymer configuration would drastically change according to the shear rate. Such critical behavior (and hysteresis) of the coil-stretch transition was first argued by de Gennes.[40] An example of such hysteresis was reported by Schroeder *et al.* for a very long DNA ($L \approx 1.3$ mm) in a cross-slot experiment.[9,41,42] In their experiment, no hysteresis was observed for DNA up to 575 μm long.

In the present theoretical calculation, no discontinuous behavior was found for DNA 1.3 mm long with fully penetrating flow. For a very long DNA, it is considered that hydrodynamic nonlocal interactions play a significant role in inducing hysteresis.[42] On the other hand, as shown in Fig. 5, the coil-stretch transition can become discontinuous by a slight modification of the force field applied to the chain. This indicates the possibility that a relatively short DNA can exhibit a discontinuous coil-stretch transition under the application of a suitable flow field.

Hysteresis has also been reported for a medium-length chain through a 4:1:4 contraction-expansion channel using molecular dynamics simulations.[43] In this case, asymmetric flow patterns appear with increasing Deborah number, and thus, a polymer molecule is exposed to very different flow fields during elongation and shrinking. Another factor that can influence microfluidics is the quality of the wall surface. In this context, flow through a periodic waving channel has been investigated.[44–46] Tsouka *et al.* reported that asymmetric flow arises on a waving substrate with an increase in the polymer concentration.[47] Therefore, careful consideration is necessary to associate the presence of hysteresis with a first-order transition.

V. CONCLUSIONS

The flow profile was examined near the connection between a large inlet pool and a narrow channel (Fig. S3 in the supplementary material). Due to the abrupt narrowing of streamlines at the connection, fluid is greatly accelerated near this point. The width of the acceleration region is on the order

of the channel width. The profile of the flow speed along the channel axis can be approximated by a sigmoidal function. In particular, the flow speed increases almost linearly near the connection point. The resulting shear gradient significantly elongates a DNA chain passing through the connection. The mean DNA long-axis length increases almost linearly with the flow speed and plateaus at about 300 μm/s (Fig. S1). With this system, T4 DNA is elongated by up to 70% of its entire length, on average (Fig. S1).

A coarse-grained nonlinear elastic continuous chain was solved under a constant shear rate. The theoretical results for fully penetrating flow well explain the experimental results. Thus, we conclude that DNA stretching near the junction is induced by the shear rate along a streamline. Flow that is fully penetrable to a DNA molecule of the present size and a one-dimensional model represents a reliable analytical method for understanding the mechanism of stretching of a giant polymeric molecule. In particular, the present model calculation is expected to provide a useful tool for the design of flow fields to produce a desired stretching effect on genome-sized DNA.

SUPPLEMENTARY MATERIAL

See supplementary material for additional details on: S1. Comparison of DNA elongations with/without glycerol, S2. The overstretching of DNA molecule, S3. Estimation of a force applied to DNA molecule, S4. Measurement of flow speed profiles, and S5. Observation of conformational change of DNA molecules.

ACKNOWLEDGMENTS

This work was supported by JSPS KAKENHI, Grant Nos. 25790030, 15H02121, 25103012, and 18K06175.

[1]L. Guillou, J. B. Dahl, J.-M. G. Lin, A. I. Barakat, J. Husson, S. J. Muller, and S. Kumar, Biophys. J. **111**, 2039 (2016).
[2]K. Hirano, Y. Matsuzawa, H. Yasuda, S. Katsura, and A. Mizuno, J. Capillary Electrophor. Microchip Technol. **6**, 13 (1999).
[3]D. J. Berard, M. Shayegan, F. Michaud, G. Henkin, S. Scott, and S. Leslie, Appl. Phys. Lett. **109**, 033702 (2016).
[4]D. Kim, C. Bowman, J. T. Del Bonis-O'Donnell, A. Matzavinos, and D. Stein, Phys. Rev. Lett. **118**, 048002 (2017).
[5]S. Gholizadeh, M. S. Draz, M. Zarghooni, A. Sanati-Nezhad, S. Ghavami, H. Shafiee, and M. Akbari, Biosens. Bioelectron. **91**, 588 (2017).
[6]N. K. Mani, S. Rudiuk, and D. Baigl, Chem. Commun. **49**, 6858 (2013).
[7]H. Mori, K. O. Okeyo, M. Washizu, and H. Oana, Biotechnol. J. **13**, 1700245 (2018).
[8]S. Sachdev, A. Muralidharan, and P. E. Boukany, Macromolecules **49**, 9578 (2016).
[9]E. S. G. Shaqfeh, J. Non-Newtonian Fluid Mech. **130**, 1 (2005).
[10]A. A. Kurganov, F. Svec, and A. Y. Kanateva, Polymer **60**, A1 (2015).
[11]T. M. Fischer, M. Stohr-Lissen, and H. Schmid-Schonbein, Science **202**, 894 (1978).
[12]F. Durst, R. Haas, and W. Interhal, Rheol. Acta **21**, 572 (1982).
[13]P. N. Dunlap and L. G. Leal, J. Non-Newtonian Fluid Mech. **23**, 5 (1987).
[14]M. J. Menasveta and D. A. Hoagland, Macromolecules **24**, 3427 (1991).
[15]T. T. Perkins, D. E. Smith, R. G. Larson, and S. Chu, Science **268**, 83 (1995).
[16]J. Marko and E. Siggia, Macromolecules **28**, 8759 (1995).
[17]L. Oliveria and M. S. Rocha, Phys. Rev. E **96**, 032408 (2017).
[18]T. T. Perkins, D. E. Smith, and S. Chu, Science **276**, 2016 (1997).
[19]D. E. Smith and S. Chu, Science **281**, 1335 (1998).
[20]D. E. Smith, H. P. Babcock, and S. Chu, Science **283**, 1724 (1999).
[21]P. LeDuc, C. Haber, G. Bao, and D. Wirtz, Nature **399**, 564 (1999).
[22]H. P. Babcock, R. E. Teixeira, J. S. Hur, E. S. G. Shaqfeh, and S. Chu, Macromolecules **36**, 4544 (2003).
[23]R. Marie, J. N. Pedersen, D. L. V. Bauer, K. H. Rasmussen, M. Yusuf, E. Volpi, H. Flyvbjerg, A. Kristensen, and K. U. Mir, Proc. Natl. Acad. Sci. U. S. A. **110**, 4893 (2013).
[24]J. N. Pedersen, R. Marie, A. Kristensen, and H. Flyvbjerg, Phys. Rev. E **93**, 042405 (2016).
[25]K. Günther, M. Mertig, and R. Seidel, Nucleic Acids Res. **38**, 6526 (2010).
[26]M. Maaloum, P. Mullera, and S. Harlepp, Soft Matter **9**, 11233 (2013).
[27]P. S. Doyle, E. S. G. Shaqfeh, G. H. McKinley, and S. H. Spiegelberg, J. Non-Newtonian Fluid Mech. **76**, 79 (1998).
[28]L. Li and R. G. Larson, Macromolecules **33**, 1411 (2000).
[29]J. Wang and C. Lu, J. Appl. Phys. **102**, 074703 (2007).
[30]C. Bustamante, Z. Bryant, and S. B. Smith, Nature **421**, 423 (2003).
[31]A. R. Khokhlov, A. Y. Grosberg, and V. S. Pande, *Statistical Physics of Macromolecules* (American Institute of Physics, New York, 1994).
[32]T. T. Perkins, S. R. Quake, D. E. Smith, and S. Chu, Science **264**, 822 (1994).
[33]T. Iwaki, T. Ishido, K. Hirano, A. A. Lazutin, V. V. Vasilevskaya, T. Kenmotsu, and K. Yoshikawa, J. Chem. Phys. **142**, 145101 (2015).
[34]A. Celani, A. Puliafito, and D. Vincenzi, Phys. Rev. Lett. **97**, 118301 (2006).
[35]S. Gerashchenko and V. Steinberg, Phys. Rev. E **78**, 040801 (2008).
[36]T. Odijk, Polymers **9**, 190 (2017).
[37]D. Kivotides, V. V. Mitkin, and T. G. Theofanous, J. Non-Newtonian Fluid Mech. **161**, 69 (2009).
[38]J. Tang, D. W. Trahan, and P. S. Doyle, Macromolecules **43**, 3081 (2010).
[39]D. Panja, G. T. Barkema, and J. M. J. van Leeuwen, Phys. Rev. E **93**, 042501 (2016).
[40]P. G. De Gennes, J. Chem. Phys. **60**, 5030 (1974).
[41]C. M. Schroeder, H. B. Babcock, E. S. G. Shaqfeh, and S. Chu, Science **301**, 1515 (2003).
[42]C. M. Schroeder, E. S. G. Shaqfeh, and S. Chu, Macromolecules **37**, 9242 (2004).
[43]J. Castillo-Tejas, A. Rojas-Morales, F. Lòpez-Medina, J. F. J. Alvarado, G. Luna-Bàrcenas, F. Bautista, and O. Manero, J. Non-Newtonian Fluid Mech. **161**, 48 (2009).
[44]A. Cabal, J. Szumbarski, and J. M. Floryan, Comput. Fluids **30**, 753 (2001).
[45]H. Keramati, A. Sadeghi, M. H. Saidi, and S. Chakrabortiy, Int. J. Heat Mass Transfer **92**, 244 (2016).
[46]L. Martìnez, O. Bautista, J. Escandòn, and F. Mèndez, Colloids Surf., A **498**, 7 (2016).
[47]S. Tsouka, Y. Dimakopoulos, and J. Tsamopoulos, J. Non-Newtonian Fluid Mech. **228**, 79 (2016).